Development of High-Speed Data Acquisition Triggering System for Hypersonic Wind Tunnel Applications

Elijah J. LaLonde[1], Valeria Delgado Elizondo[2], and Christopher S. Combs[3]

The University of Texas at San Antonio, San Antonio, TX, 78249

The rapid increase in hypersonic aerothermodynamic research in high-speed wind tunnel facilities poses the need for the development and utilization of high-speed data acquisition devices with fast sensing and triggering capabilities, particularly when nonintrusive measurement techniques are being employed. Similar to other wind tunnel facilities in the nation such as the Purdue Mach 6 and University of Arizona Mach 4 facilities, the Mach 7 Ludwieg Tube at the University of Texas at San Antonio (UTSA) uses a diaphragm rupture mechanism to initiate test runs in the facility. The manufacturing process of the diaphragms among other contributors can introduce a factor of uncertainty as to the moment and the pressure at which rupture occurs, particularly in the early stages of testing. In these high-speed wind tunnels, the window for collecting data can be on the order of only a few hundred milliseconds. Consequently, the need for high-speed triggering of data acquisition systems to fully utilize the short test times is of utmost importance. A simple, compact, and cost-effective system was developed, employing a pressure transducer and an Arduino microcontroller that is able to activate the data acquisition systems with a pressure drop of 36.86 kPa $\pm$ 4.62 kPa (5.346 psi $\pm$ 0.67 psi). Several variables play a role in determining the hardware time delay of the developed system, but the maximum delays of the module are on the order of 200 microseconds. The time from diaphragm burst to the start of data acquisition is 9.78 ms $\pm$ 0.5 ms. This system not only enables capturing the phenomena of interest but also offers the potential to aid in the optimization of data file size. The time delay measurements associated with the different hardware were measured via an oscilloscope and an internal Arduino time function. This paper presents the time delays, circuitry, costs, and limitations of this triggering unit. Schlieren images featuring the shock wave produced after diaphragm rupture are also shown as proof of concept. Successful diaphragm tests at varying burst pressures have proven that the devised system is reliable and leads to repeatable triggering of hardware and data acquisition in high-speed applications.

Nomenclature

a	=	Speed of sound (m/s)
γ	=	Ratio of specific heats
R_{air}	=	Ideal gas constant of air (J/kg · K)
T	=	Absolute Ambient Temperature (K)
α	=	Current to pressure conversion (kPa/A)
β	=	Voltage step-size of the ADC process (V/step)
ΔP_{DT}	=	Trigger Pressure Threshold (kPa)

[1] Graduate Research Assistant, Department of Mechanical Engineering, AIAA Student Member.
[2] Graduate Research Assistant, Department of Mechanical Engineering, AIAA Student Member.
[3] Dee Howard Endowed Assistant Professor, Department of Mechanical Engineering, Senior AIAA Member.

ΔP_A = Trigger Pressure Threshold (Dimensionless)
R = Resistance (Ω)

I. Introduction

The rise in hypersonic aerothermodynamic research with applications in the development of hypersonic commercial flights [1], space missions [2], and advancement of aerospace defense [2] has led to a surge in high-speed wind tunnel facilities in both academia and industry [3,4,5]. These facilities that use non-intrusive measurement techniques require reliable and versatile high-speed triggering devices to activate these data acquisition (DAQ) systems. The University of Texas at San Antonio (UTSA) has a Ludwieg Tube Mach 7 Wind Tunnel in its last stage of construction and is undergoing preliminary testing [6,7]. Different methods that have been previously used to initiate impulse facility test runs are fast-acting valves [8], multiple stage diaphragms [9] and single diaphragms [10]. The Mach 7 Ludwieg Tube at UTSA currently uses the latter of the configurations. The first two methods allow for more control of the moment and pressure at which tests begin, enabling to prepare hardware and DAQ systems for activation and synchronization. On the other hand, single stage diaphragms inherently have a higher uncertainty in burst pressure due to their reliance on the manufacturing process and other factors [11]. This uncertainty is even more significant in the early stages of testing when different diaphragm configurations involving score patterns, depths, material, and thickness are under investigation.

The total duration of wind tunnel tests at speeds greater than Mach 5 tend to be on the order of milliseconds (ms) [6]. Therefore, there is a need to develop a fast-sensing triggering system to activate hardware as quickly as possible after diaphragm rupture to provide enough time to collect statistically significant data trends. Initiating DAQ devices with fast sensing systems is also beneficial for data file size optimization as these systems typically run on the order of several kilohertz (kHz) and produce large data files [12]. To satisfy the requirements of this application, a simple and cost-effective system was developed. This high-speed triggering system utilizes a pressure transducer located upstream of the wind tunnel driver tube and senses a pressure drop from the expansion wave that is produced upon diaphragm rupture. The analog signal is processed by an Arduino Uno R3 microcontroller that triggers equipment such as a high-speed camera and high-energy laser, allowing for data collection of Schlieren images, particle imaging velocimetry (PIV), and planar laser induced fluorescence (PLIF). These non-intrusive measurement techniques are common in hypersonic flow diagnostics [13,14] and need to be initiated when wind tunnel test runs begin. This paper presents detailed information on the hardware that was employed, the circuit configuration, the costs associated with the device and the results of the various time delays along with the limitations of this triggering module. Multiple successful diaphragm tests at varying burst pressures validate the reliability of the system to trigger measurement devices in high-speed applications.

II. Experimental Program

A. Experimental Facility

The UTSA Mach 7 Ludwieg Tube Wind Tunnel facility, where tests were performed, pressurizes the working fluid with a MAX-AIR 35 electric compressor with a 4.2 SCFM charge rate [6]. A steady pressurization rate of ~68.95 kPa/min was observed. The 18.29 m (60 ft) driver tube is rated for a max pressure of 13.79 MPa (2000 psia) and is equipped with six Omega pressure transducers along the driver tube length [6]. The triggering pressure transducer was added next to the pressure transducer located nearest to the diaphragm. The Mach 7 Ludwieg Tube at UTSA is presently equipped with Omega Pressure Transducers (PX319-3KGI) with a range of 1 standard atmosphere to 20.79 MPa (3000 psig) on the driver tube. The triggering pressure transducer has a balance of 4.003 mA and a sensitivity of 15.962 mA. The pressure transducer employed to sense the pressure drop to activate the hardware is located 1.41 m (55.5 inches) from inlet of the expansion section upstream of the driver tube and it has a response time of <1 ms. The UTSA Hypersonics Facility can be found below in Fig. 1. A Piping and instrumentation diagram (P&ID) of the UTSA Mach 7 Wind Tunnel can be found in Ref. 7.

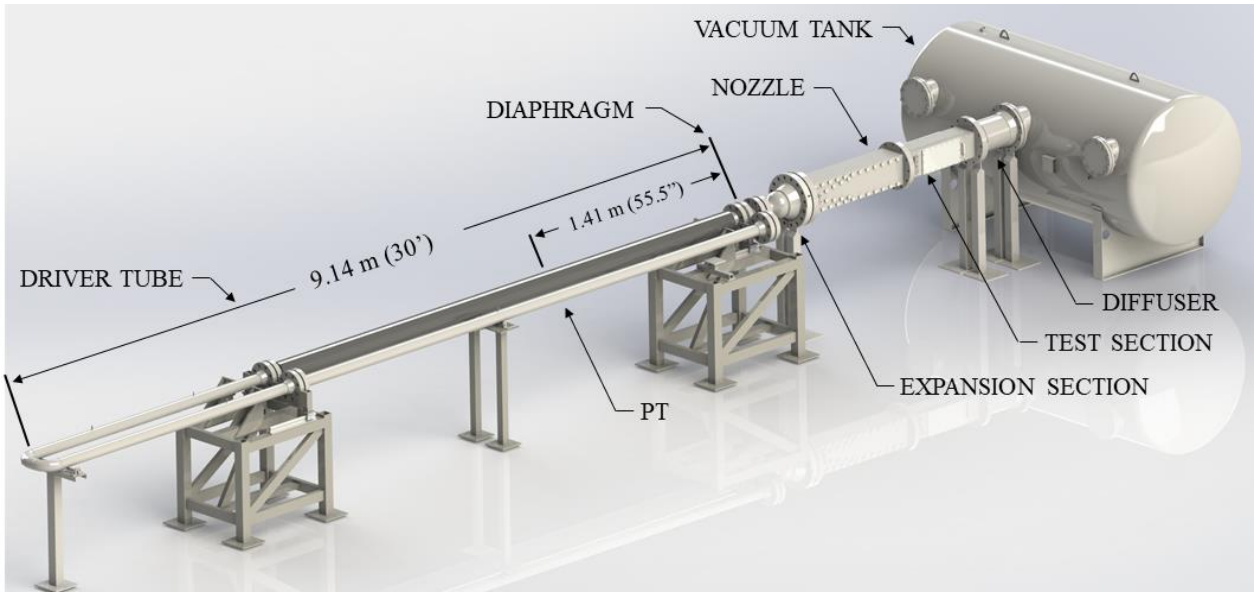

Figure 1: Rendering of the Mach 7 Ludwieg Tube Wind Tunnel Facility at UTSA.

B. Circuitry Development

The working principle of the device is based on tracking the propagation of the expansion wave created when a diaphragm ruptures and using the resulting pressure change to trigger operations. Ohms' law and a Resistor-Capacitor (RC) low pass filter were used in the design of the circuit to convert the current signal from the pressure transducer to a voltage reading that the microcontroller can process. A low pass filter was adopted to reduce noise in the pressure transducer signal to avoid accidental triggering and consequently allowing the pressure threshold to be lowered. The mathematical model for the final triggering pressure threshold is provided as follows:

$$\Delta P_{DT} = \frac{\alpha \cdot \Delta P_A \cdot \beta}{\mathrm{R}} \tag{1}$$

Where α is the current to pressure conversion factor using the ratio of the pressure-current range. β is the analog voltage step size given by the ratio of the maximum voltage of the microcontroller, to the 1024 steps in the 10 bit analog to digital conversion (ADC) process. R represents the resistance in Ohms for the second resistor (700 Ω) as seen in Fig. 2. The circuit implements an RC low pass filter with two resistors of 200 and 700 Ohms respectively, a 1 μF capacitor and terminals to connect multiple measurement devices. A circuit diagram and rendering are shown below.

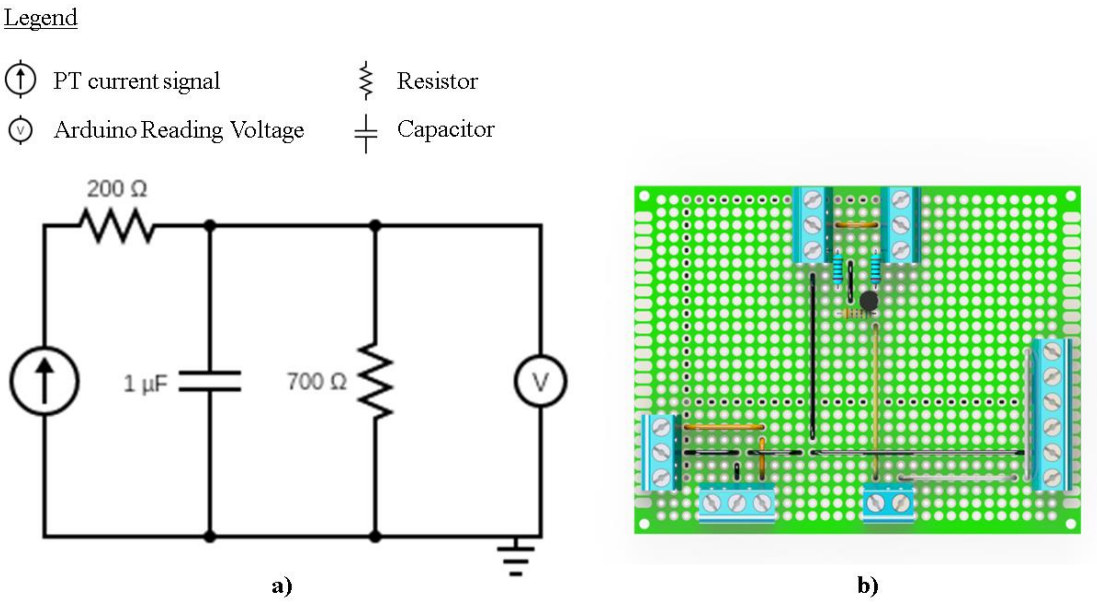

Figure 2: a) Circuit diagram of the designed circuit and b) Rendering of it on a PCB board.

A 12 V signal from an Astro-MED external power supply travels across the two terminals at the top of the circuit board in Fig. 2b to power the pressure transducer. The current signal coming from the pressure transducer passes through the lowpass filter and is measured by the Arduino. The finished module is displayed in Fig. 3.

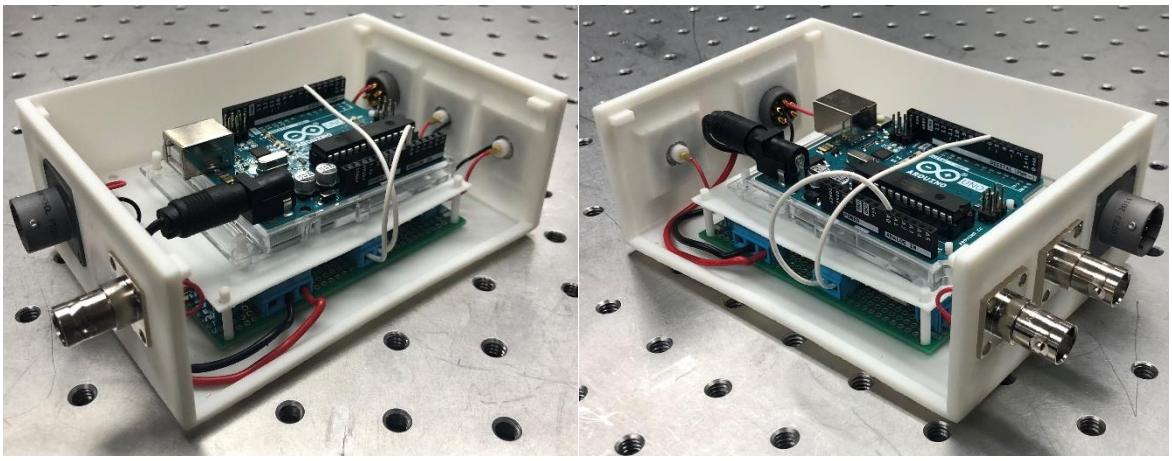

Figure 3: Assembled triggering module without box lid.

The circular military standard (MIL) spec connector at the top left of the circuit box brings the 12 V signal from the external power supply into the module to power the pressure transducer. Similarly, the BNC connection on the left side also supplies a 12 V signal to the microprocessor. The MIL spec connector on the right connects to the triggering pressure transducer. All the BNC connections on the right of the box are signal outputs, used for triggering DAQ hardware. Figure 4 outlines the experiment used for prototyping the circuit.

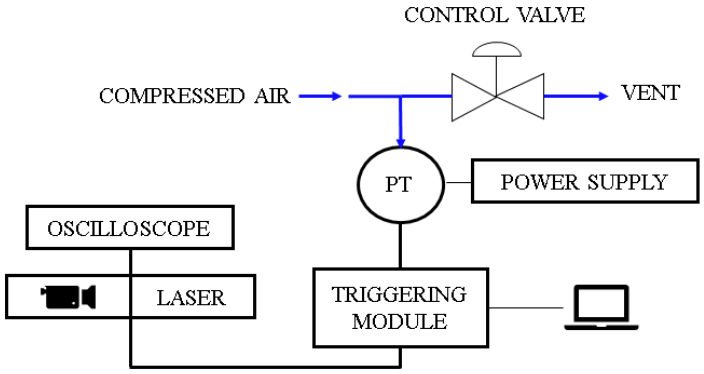

Figure 4: P&ID of the setup used in developing the circuit.

A small volume of air was pressurized and released using a hand valve. The parameters of the module were tuned so that opening the hand valve would trigger the module and DAQ hardware. This setup simulates the diaphragm rupture test in the wind tunnel on a smaller scale. The flexibility of the setup allowed for iterating efficiently, until optimal parameters were found for the experiment.

C. Measurement of Hardware Delays

The time delays associated with the reception and output of electric signals to activate and synchronize hardware were measured utilizing a Teledyne LeCroy 200 MHz Oscilloscope. The trigger (TTL IN), record (REC) and synchronization (SYNC) signals from the high-speed camera were used to measure time delays between the signals, using the triggering signal from the Arduino as the reference time. The experiment implemented two configurations, Arduino-Camera and Arduino-Camera-Laser. In the first configuration, the microcontroller triggered the camera, while in the later, the Arduino signal triggered the laser which then would activate the camera. The experiment was repeated for multiple acquisition rates to obtain data of the delays as a function of frequency. The signal processing time of the microcontroller itself was retrieved using a built-in function in the Arduino program.

D. Validation Experiment

Compressible flow literature identifies the phenomena observed in a Ludwieg Tube as a shock tube case and provides a thorough explanation of the gas behavior for the conditions in this application [15]. The UTSA Mach 7 Wind Tunnel can be modeled as a shock tube with a high and a low-pressure region separated by a diaphragm. Upon diaphragm burst, a normal shock will be produced in the direction of the low-pressure region and an expansion wave will travel in the opposite direction at the local speed of sound. Air flow within the driver tube can be classified as isentropic and the ideal gas model is a valid assumption [15]. The speed of sound is then given by Eq. (2) below.

$$a = \sqrt{\gamma R_{air} T} \tag{2}$$

Where a is the local speed of sound, γ is the ratio of specific heats for air as a working fluid, R_{air} represents the ideal gas constant in mass base and T is the absolute ambient temperature. The expansion wave's propagation time to the triggering pressure transducer can be calculated using this isentropic assumption.

Schlieren is a visualization technique that is often used to capture the flow density gradients, enabling to record fluid phenomena [16]. Capturing the initial shock after diaphragm burst, traveling faster than the speed of sound validates the efficiency of the triggering device in this high-speed application. The Schlieren was set up in a Z-type configuration employing two 15.24 cm (6-inch) diameter concave spherical mirrors. A flat mirror was used so that the camera could be located further away from the test area, ensuring no damage could occur in the case of diaphragm failure. Finally, the light was filtered utilizing a razor blade to obtain Schlieren while the images were recorded with a Photron SA-Z Fast Cam at a frame rate of 50.4 kHz. Figure 5 displays the Schlieren set up for the diaphragm test.

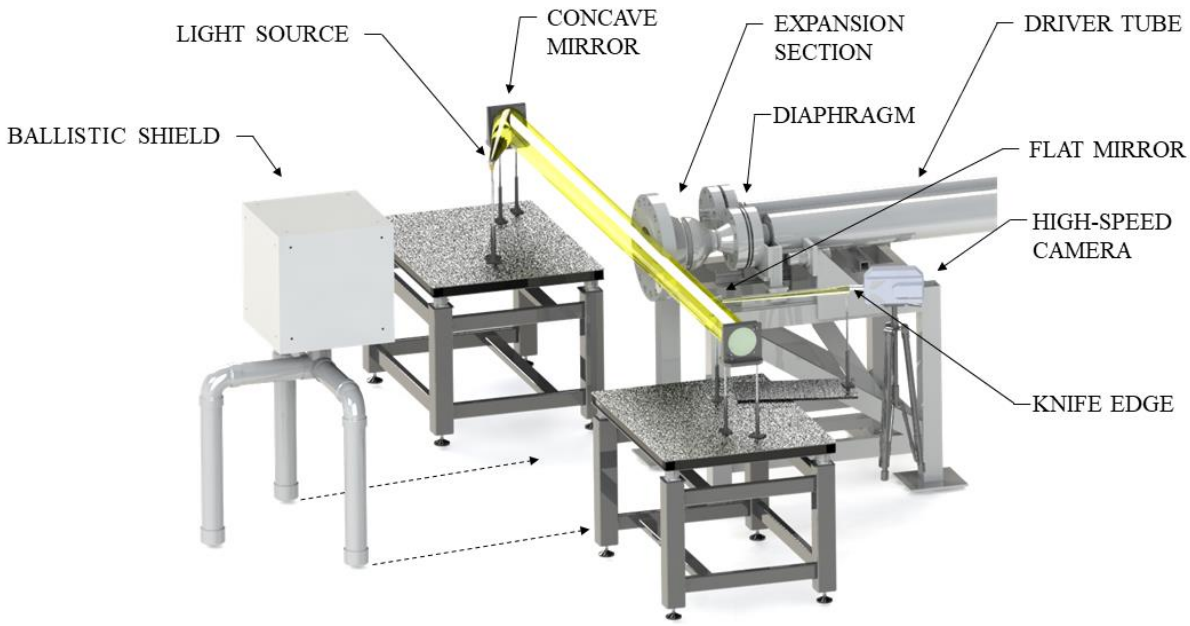

Figure 5: Schlieren Z-setup for diaphragm testing. Dashed lines indicate where the ballistic shield was installed for the test.

The diaphragm used in the validation experiment was an A 3105 grade Aluminum diaphragm with 3.44 inch bore size and thickness of 0.019 inches, manufactured in-house. This diaphragm is designed for low pressures up to 1.48 MPa (200 psig), and cold burst at room temperature. As this style of diaphragm is in its final stages of testing, the nozzle, test section and diffuser were not connected as a safety measure against potential shrapnel. As such, the expansion section was exhausted to atmosphere. For additional safety measures, a ballistic shield was used to catch any potential shrapnel in case of failure.

III. Results

Several variables went into determining the time delays of this system. These include the analog to digital conversion time of the pressure transducer signal, logic processing time of the Arduino microcontroller, and the reaction time of the device to generate the signal. The Arduino hardware delay to perform the ADC of the pressure transducer signal and determine whether the pressure had dropped below the set threshold value was found to be 112 μs using the micros Arduino function. This micros function takes 4 μs to generate a time stamp, which was considered in the Arduino delay measurement. The Arduino time delay did not fluctuate throughout the trial runs and could be reduced if the analog pin receiving the signal is called directly as opposed to using the prebuild analogRead function. However, directly calling the pin was found to produce inherently noisier readings. For that reason, it was decided that even though it is approximately 10x faster to read the pins directly than using the analogRead function, it was more beneficial to produce a cleaner signal at the cost of an extra 100µs delay. Table 1 displays a breakdown of the internal Arduino delays.

Function:	**Delay:**
micros()	4 μs
analogRead()	108 μs
Logic Processing	4 μs
Total Arduino Delay:	112 μs

Table 1: This table outlines the delays of the Arduino Uno. Each function takes a certain number of lines for the microprocessor to read and so they do not fluctuate.

With the analogRead function and the designed circuitry, the Arduino can trigger on a change of 4 ADC steps, which corresponds to a pressure drop of 36.86 kPa ± 4.62 kPa (5.346 psi ± 0.67 psi). The fluctuation seen in the Arduino signal was ± 1 ADC steps, yet, to ensure no accidental triggering of the system, the value of 4 ADC steps was selected. Figure 6 shows the sequence of events that occur during a wind tunnel run.

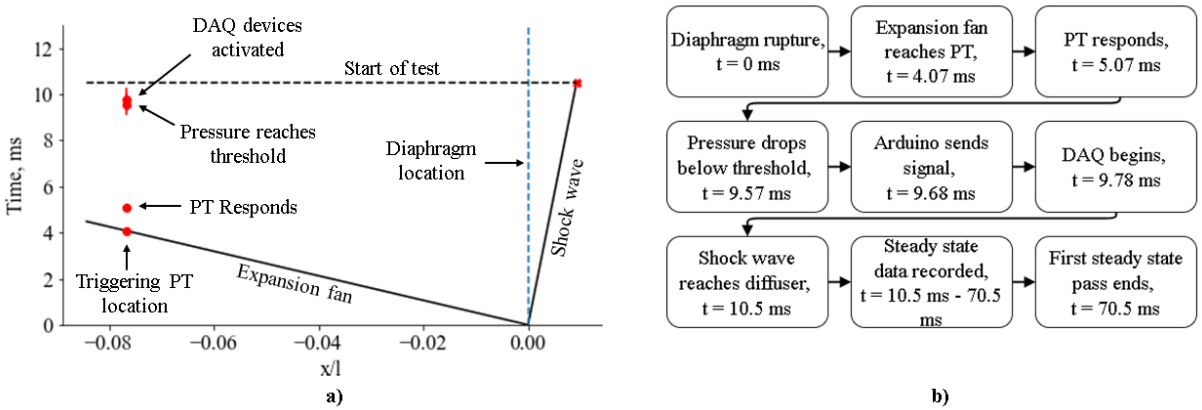

Figure 6: a) x-t diagram of the beginning of a wind tunnel run b) Block diagram sequence of events.

This figure highlights the effectiveness of the DAQ triggering system. The assumption that the first steady state pass begins when the shock wave reaches the diffuser (t = 10.5 ms) is a very conservative estimate. Flow is expected to reach steady state condition at t > 10.5 ms. Accounting for the uncertainty in the pressure threshold, this module can trigger DAQ systems and begin recording data before the first steady state pass begins.

A. Frequency Dependence

The response of the high-speed camera and laser synchronized together is strongly dependent on the acquisition frequency. Figure 7 shows the frequency dependence on the camera response time.

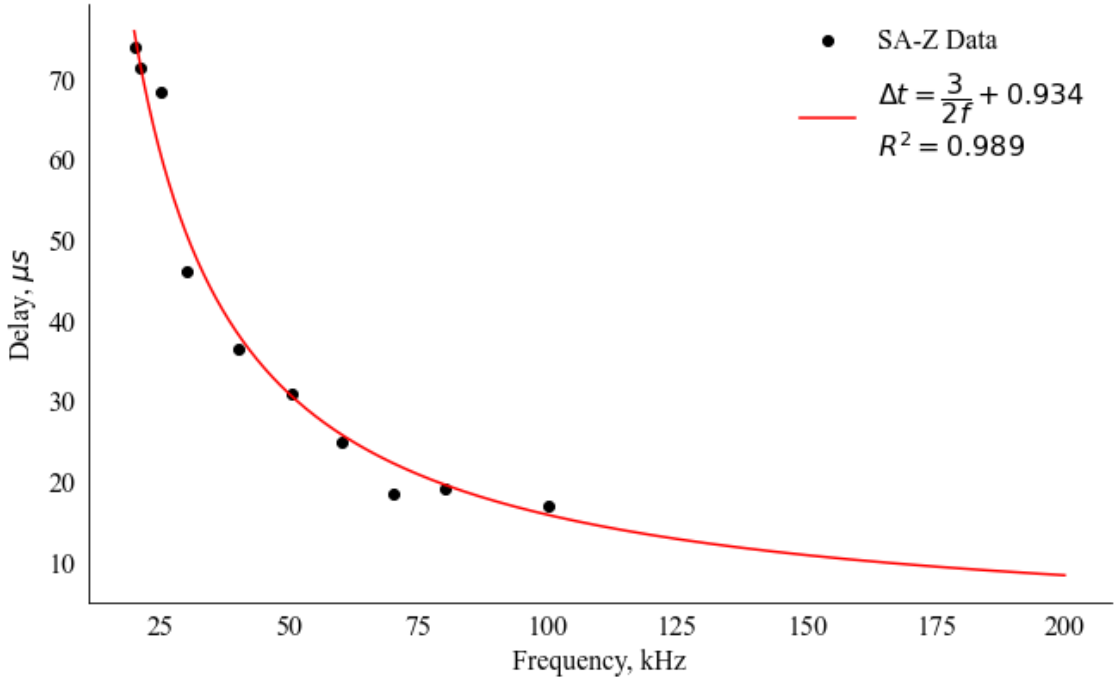

Figure 7: SA-Z frequency response at various acquisition frequencies.

As expected, higher the acquisition frequency, produce faster the system responses. The fluctuation in the camera response time is due to the way it is programmed to respond to a triggering signal. The internal clock of the SA-Z is continuously running. Regardless of when the TTL IN signal is sent, the camera only starts recording after the second SYNC signal pulse. This trend is illustrated in Fig. 8 below.

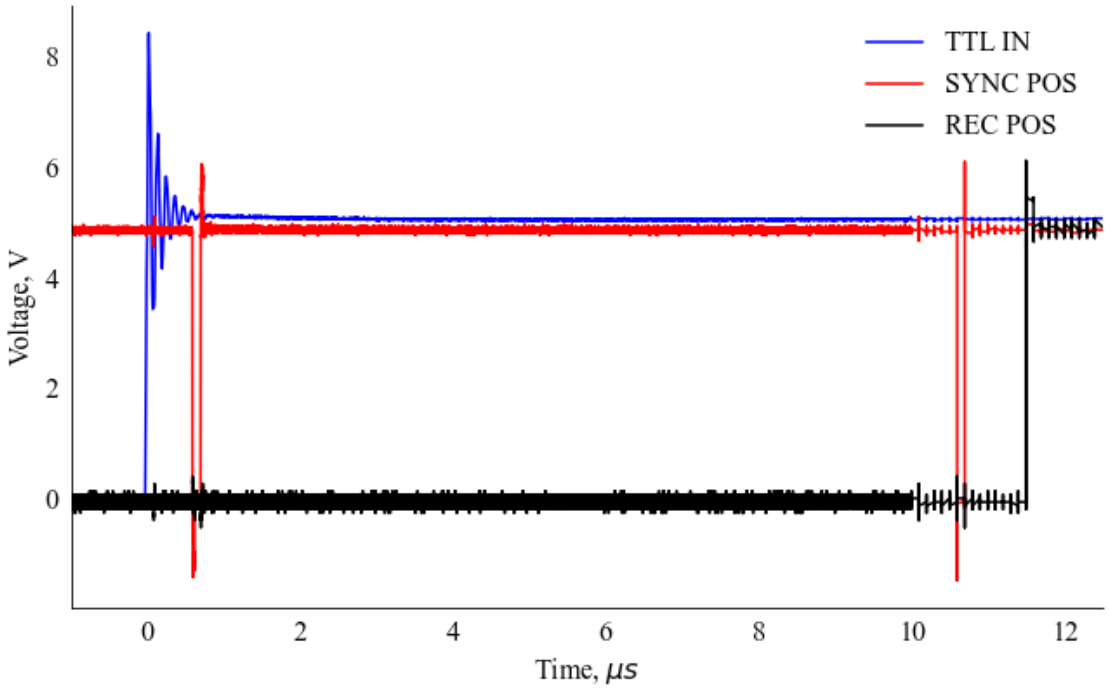

Figure 8: SA-Z signal pulses at 100 kHz acquisition frequency after triggering.

Figure 8 explains the large fluctuation in the camera's response time and frequency dependence. At higher frequencies, the SYNC pulse train is closer together, resulting in a faster response. If the TTL IN signal is received right after one of the SYNC pulses, there will be a larger time delay. The constant offset of the frequency curve (Fig. 7) was found from taking the average offset between the REC positive signal and the second SYNC pulse at every frequency. The uncertainty of the delays is $1/f$. The uncertainty of all data points shown in black in Fig. 4 fall within this uncertainty. The R^2 value of 0.989 gives confidence in the SA-Z frequency response model. No other major delays were observed when the camera and laser were synchronized together. The time required for the laser to mirror the triggering signal to the camera is 3.63 $\mu s \pm 0.14\ \mu s$.

B. Pressure Transducer Considerations

The main factor that should be considered in minimizing time delays is the pressure transducer's physical location on the wind tunnel. Currently, the pressure transducer is located 1.41 m (55.5 inches) from the diaphragm. When the diaphragm ruptures, the expansion fan will travel back through the driver tube [7] and this pressure wave is what triggers the module. To minimize the time between diaphragm rupture and the expansion wave reaching the pressure transducer, it is best to have the triggering pressure transducer located as close to the diaphragm as possible. The present location of the pressure transducer is as close to the diaphragm as possible when the nozzle and test section are not connected to the wind tunnel. With the nozzle and test section in place for wind tunnel tests, the pressure transducer can be placed on the expansion section on the low-pressure side of the diaphragm [7] and the Arduino can trigger off a rise in pressure when the tests begin. As the expansion section is 70.49 cm (27.75 inches), it is anticipated that this system will be also able to trigger the data acquisition hardware before the first steady state pass occurs in the test section. It should be noted that while this system currently triggers off a drop in pressure, it can just as easily trigger off an increase in pressure with a simple switch of logic in the Arduino code, without changing the internal delay of the microprocessor.

C. Schlieren Images from Diaphragm Test

As proof of concept and as the final stage of testing for this system, the triggering module was used to trigger the SA-Z and get Schlieren images of the flow exiting the expansion section into the atmosphere. Because the end of the expansion section is closer to the diaphragm than the triggering pressure transducer, a middle trigger on the camera was used so that the start of the rupture could still be captured. With a middle trigger, the camera starts recording when it is switched to ready and then uses the trigger signal as the midpoint of the recording, saving images taken before and after the triggering signal. A middle trigger works excellently for a Schlieren setup; however, this method does not work when using the laser system in conjunction with the SA-Z. An array of Schlieren images is shown below for a diaphragm test.

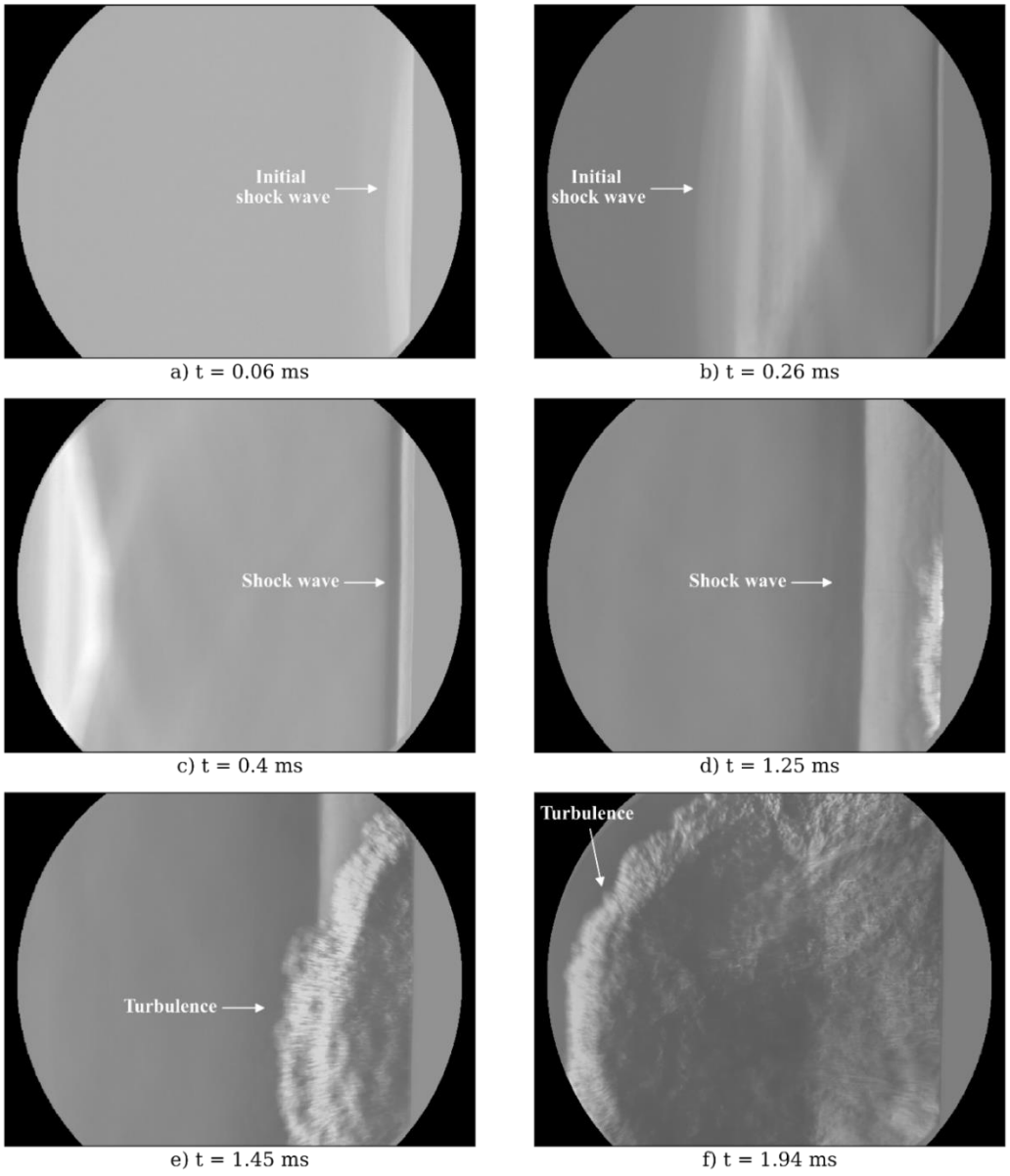

Figure 9. Schlieren images with background subtraction of the diaphragm rupture collected at 50.4 kHz. Burst pressure of 406.8 kPa (59 psia).

Data from this test (Fig. 9) demonstrates the triggering system's capabilities when incorporated into the wind tunnel facility and its ability to reliably trigger the camera to acquire data.

D. System Costs

The developed triggering system is economical and cost effective. The most expensive part of the module is the Arduino Uno R3 ($22.00). The 200 Ω resistors used in the circuit have a 0.1% uncertainty and cost $1.65 each. The 500 Ω resistor, also 0.1% uncertainty costs $0.929. Using resistors with a low tolerance is the most important aspect of this circuit, as the uncertainty of the pressure drop is largely determined by the tolerance of the resistance. There is no such constraint for the capacitor since its sole purpose is to filter the signal. Its tolerance impacts the cutoff frequency of the low pass filter, but it does not impact the uncertainty of the pressure drop. The capacitor used was an off the shelf 1 μF capacitor. All other aspects of the designed circuit are up to the designers, such as connectors and terminals for both the circuit and the box. The connectors used for this particular system were two circular MIL spec connectors ($6.99 each) and three coaxial connectors ($4.51 each). The entire system totals under $100, making it cost efficient to prototype and build.

E. Plans for Improvement

This timing circuit is an easy, cost efficient solution for triggering high-speed data acquisition hardware. There are limitations of this circuit due to the 10-bit resolution and 5V max input of the Arduino. The present circuit can read pressures up to 1.48 MPa (200 psig) with a 4-20 mA PX319-3KGI pressure transducer. The Mach 7 Ludwieg Tube facility at UTSA can reach pressures of up to 13.79 MPa (2000 psia) [6]. In the early stages of the Mach 7 build, test pressures will not exceed 1.48 MPa (200 psig). However, there are various ways to make the circuit work for pressures higher than 1.48 MPa (200 psig). The first way is to build another circuit with different resistances. Because the system reads a pressure transducer that outputs a current signal, resistors can be chosen so that the Arduino reads its max of 5V at any pressure desired. The other solution is to select another microcontroller with a better ADC resolution. The later solution is preferred. The ESP-32S is an excellent candidate to replace the Arduino as it has 12-bit ADC resolution and costs less than the Arduino Uno ($10.99). Even though it can only read voltages up to 3.3V, the 12-bit resolution would allow it, with proper resistor values, to read from 1 standard atmosphere to 13.79 MPa (0-2000 psia) and still be able to detect pressure changes smaller than the present circuit with the Arduino.

It was previously stated that this system has the potential for data file size optimization. In high-speed wind tunnel testing, significantly large data acquisition rates are required. For example, the UTSI Mach 4 Ludwieg Tube uses sampling rates of 50 kHz [12]. Without data file size optimization, file sizes can get too large to be practical. With this timing circuit, a digital signal can be sent to LabView to begin saving data when the diaphragm ruptures and consequently, reduce data file sizes.

IV. Conclusion

In this work, a high-speed data acquisition triggering system was developed and characterized. It has shown excellent results for reliably triggering systems on the UTSA Mach 7 Ludwieg Tube facility. The system can detect a change of 36.86 kPa $\pm$ 4.62 kPa (5.346 psi $\pm$ 0.67 psi) with a time delay of less than 200 ms due to the module and the camera/laser system. The time from diaphragm rupture to the start of data acquisition was found to be 9.78 ms $\pm$ 0.5 ms, including expansion wave travel time. The triggering module can initiate data acquisition before steady state flow is achieved in the test section. Using a strategically placed pressure transducer, it is believed that this system can easily be incorporated into more hypersonic aerothermodynamic applications needing high-speed data acquisition triggering. The versatility, simplicity, and cost effectiveness of this system makes it appealing for meeting such needs. While other systems may use data acquisition hardware different than the Photron SA-Z with varying lag times, it is safe to assume that similar data acquisition systems should exhibit comparable response times as the DAQs tested for the Mach 7 Ludwieg Tube facility at UTSA. When developing this system for hypersonic applications, it is recommended to go straight into using an ESP-32S microcontroller because of the advantages that were previously laid out. The only modifications to the circuitry developed in this application are different resistors.

Acknowledgments

This work was sponsored (in part) by the Air Force Office of Scientific Research, USAF, under grant/contract number FA9550-20-1-0190. Additional support was provided by NASA grant 80NSSC19M0194. The views and conclusions contained herein are those of the authors and should not be interpreted as necessarily representing the official policies or endorsements, either expressed or implied, of the Air Force Office of Scientific Research, NASA, or the U.S. Government. Funds for wind tunnel construction were also provided by The University of Texas at San Antonio. The authors would also like to thank Eugene Hoffman for his help and support in this process.

References

[1] Penn, J. P., and Lindley, C. A., "Space tourism optimized reusable spaceplane design." *AIP Conference Proceedings*, Vol. 387, No. 1, 1997, pp. 1073-1090.
doi: 10.1063/1.52129

[2] Chase, R. L., "Comments on a military transatmospheric aerospace plane." *AIP Conference Proceedings*, Vol. 387, No. 1, 1997, pp. 1185-1194.
doi: 10.1063/1.52112

[3] Cummings, R, and McLaughlin, T., "Hypersonic Ludwieg tube design and future usage at the US Air Force Academy." *50th AIAA Aerospace Sciences Meeting including the New Horizons Forum and Aerospace Exposition*, January 2012, p. 734.
doi: 10.2514/6.2012-734

[4] David, K., Gorham, J., Kim, S., Miller, P., and Minkus, C., "Aeronautical Wind Tunnels, Europe and Asia." LIBRARY OF CONGRESS WASHINGTON DC FEDERAL RESEARCH DIV, February 2006.

[5] Lindörfer, S. A., Anusonti-Inthra, P., Combs, C. S., Kreth, P. A., and Schmisseur, J. D., "An Investigation of the Role of an Upstream Burst Diaphragm on Flow Quality within a Ludwieg tube using RANS." AIAA Paper 2016-3801, June 2016, p. 3801. 2016.
doi: 10.2514/6.2016-3801

[6] Bashor, I., Hoffman, E., Gonzalez, G., and Combs, C. S., "Design and Preliminary Calibration of the UTSA Mach 7 Hypersonic Ludwieg Tube," AIAA Paper 2019-2859, June 2019.
doi: 10.2514/6.2019-2859

[7] Hoffman, E. N., Bashor, I. P., and Combs, C.S., "Construction of a Mach 7 Hypersonic Ludwieg Tube at UTSA," AIAA Paper 2020-2998, June 2020.
doi: 10.2514/6.2020-2998

[8] McGilvray, M., Doherty, L. J., Neely, A. J., Pearce, R., and Ireland, P., "The Oxford High Density Tunnel." AIAA Paper 2015-3548, July 2015, p. 3548.
doi: 10.2514/6.2015-3548

[9] Casper, K., Beresh, S., Henfling, J., Spillers, R., Pruett, B., and Schneider, S., "Hypersonic Wind-Tunnel Measurements of Boundary-Layer Pressure Fluctuations." AIAA Paper 2009-4054, June 2009, p. 4054. 2009.
doi: 10.2514/6.2009-4054

[10] Kimmel, R. L., Borg, M. P., Jewell, J. S., Lam, K., Bowersox, R. D., Srinivasan, R., Fuchs, S., and Mooney, T., "AFRL Ludwieg Tube Initial Performance." AIAA Paper 2017-0102, January 2017, p. 0102. 2017.
doi: 10.2514/6.2017-0102

[11] Rast, J. J., "The Design of Flat-scored High-pressure Diaphragms for use in Shock Tunnels and Gas Guns," NAVORD Report 6868, White Oak, MD, January 1961.

[12] Kreth, P. A., Gragston, M., Davenport, K., and Schmisseur, J. D., "Design and Characterization of the UTSI Mach 4 Ludwieg Tube," AIAA Paper 2021-0384, January 2021.
doi: 10.2514/6.2021-0384

[13] Combs, C. S., Lash, E. L., and Schmisseur, J. D., "Investigation of a Cylinder-Induced Transitional Shock Wave-Boundary Layer Interaction using Laser Diagnostics." AIAA Paper 2016-4321, June 2016, p. 4321.
doi: 10.2514/6.2016-4321

[14] Lash, E. L., Combs, C. S., Kreth, P. A., and Schmisseur, J.D., " Study of the Dynamics of Transitional Shock Wave-Boundary Layer Interactions using Optical Diagnostics." AIAA Paper 2017-3123, June 2017, p. 3123. 2017.
doi: 10.2514/6.2017-3123

[15] Anderson, J. D., "Modern Compressible Flow with Historical Perspective," *Unsteady Wave Motion*, 3rd ed., McGraw- Hill, New York, NY, 2003, pp. 261-266.

[16] Settles, G.S., "Schlieren and Shadowgraph Techniques: Visualizing Phenomena in Transparent Media," Springer, Berlin, 2001, pp.25-37.